Dominance of background ozone in China and its future variations under climate and emission pathways

Mengyun Li[1,2], Yang Yang[1,2*], Pinya Wang[2], Ke Li[1,2], Hong Liao[1,2]

[1]State Key Laboratory of Climate System Prediction and Risk Management/Jiangsu Key Laboratory of Atmospheric Environment Monitoring and Pollution Control/Jiangsu Collaborative Innovation Center of Atmospheric Environment and Equipment Technology/Joint International Research Laboratory of Climate and Environment Change, Nanjing University of Information Science and Technology, Nanjing, Jiangsu, China

[2]School of Environmental Science and Engineering, Nanjing University of Information Science and Technology, Nanjing, Jiangsu, China

*Correspondence to yang.yang@nuist.edu.cn

Text S1 The analysis of population-weighted ozone concentrations

Without considering future changes in disease mortality rates and population density, population-weighted concentrations reflect the potential impact of ozone on premature mortality and other health outcomes. We assess population-weighted concentrations to offer additional insights into potential exposure risks, as this metric better represents the ozone levels to which populations are actually exposed by accounting for the spatial distribution of both ozone and population. The annual mean population-weighted concentration over China is calculated following the approach.

$$Cpw = \frac{\sum_{i=1}^{N}(Pi \times Ci)}{\sum_{i=1}^{N}(Pi)}$$

where C_{PW} is the population-weighted ozone concentration; P_i and C_i represent the population density and the ozone concentration for grid cell i, respectively. Population density is fixed at 2015 levels for all scenarios (Fig. S7).

Compared to the regional average, both the population-weighted CTO (CTO_{PW}) and population-weighted CBO (CBO_{PW}) are lower over China (Fig. S14). The pattern is primarily driven by the downward transport of stratospheric ozone, which leads to higher ozone concentrations in western China, where population density is relatively low. Even after accounting for population distribution, CBO_{PW} still contributes to more than 85% of the CTO_{PW} in all scenarios, underscoring the dominant role of background ozone in determining population exposure. In the SSP1-1.9 scenario, despite emission reductions driving a downward trend in CTO, CTO_{PW} increases slightly (+1.2 ppbv relative to PD), mainly due to nonlinear ozone responses from NOx reductions, particularly in densely populated areas like the NCP, where localized ozone increases offset the expected health benefits. The CBO_{PW} decreases by 2.2 ppbv, indicating a moderate reduction in population exposure. Under SSP5-8.5, CTOPW increases significantly (+8.4 ppbv), driven largely by CBO. The growth in background ozone accounts for 63% of the increase in CTO_{PW}, showing that natural sources play a major role in elevating population exposure, regardless of emissions reductions. These results underscore the dominant role of CBO in shaping future health risks and highlight the need to consider its long-term trends in ozone control strategies.

Table S1. Reference data sources for background ozone validation.

Location	Year	Backgrounds ozone (ppbv)	Reference
NWC	2011-2014	54	Xu et al., 2020
NWC	2011-2012	53	Xu et al., 2016
NWC	2011-2014	53	Zhang et al., 2020
NWC	2011-2014	44	In this study
SWC	2011-2014	40	Xu et al., 2020
SWC	2011-2014	50	In this study
NC	2011-2014	40	Xu et al., 2020
NC	2011-2014	59	Ma et al., 2016
NC	2011-2014	39	Zhang et al., 2020
NC	2011-2014	39	Wu et al., 2022
NC	2010-2012	38	Liu et al., 2019
NC	2011-2014	39	In this study
CC	2011	45	Su et al., 2013
CC	2010-2012	31	Liu et al., 2019
CC	2011-2014	33	Zhang et al., 2020
CC	2011-2014	26	Xu et al., 2020
CC	2011-2014	35	In this study
SC	2011-2014	43	Shen et al., 2019
SC	2011-2014	39	In this study
NEC	2011-2014	31	Xu et al., 2020
NEC	2010-2012	31	Liu et al., 2019
NEC	2011-2014	37	In this study

Note: This table draws upon the data compiled in the review by Chen et al. (2025), selecting studies whose time periods encompass all or part of 2011–2014.

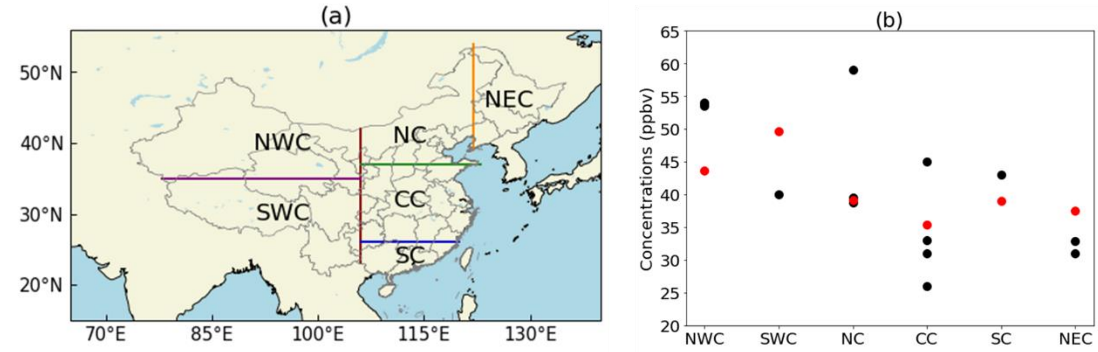

Figure S1. (a) China is divided into six regions, encompassing Northeast China (NEC), North China (NC), Centre China (CC), South China (SC), Northwest China (NWC), and Southwest China (SWC). (b) The simulated background ozone concentrations (red dots) with values reported in previous studies (black dots) during the 2011–2014 period. The literature data are compiled in Table S1.

.

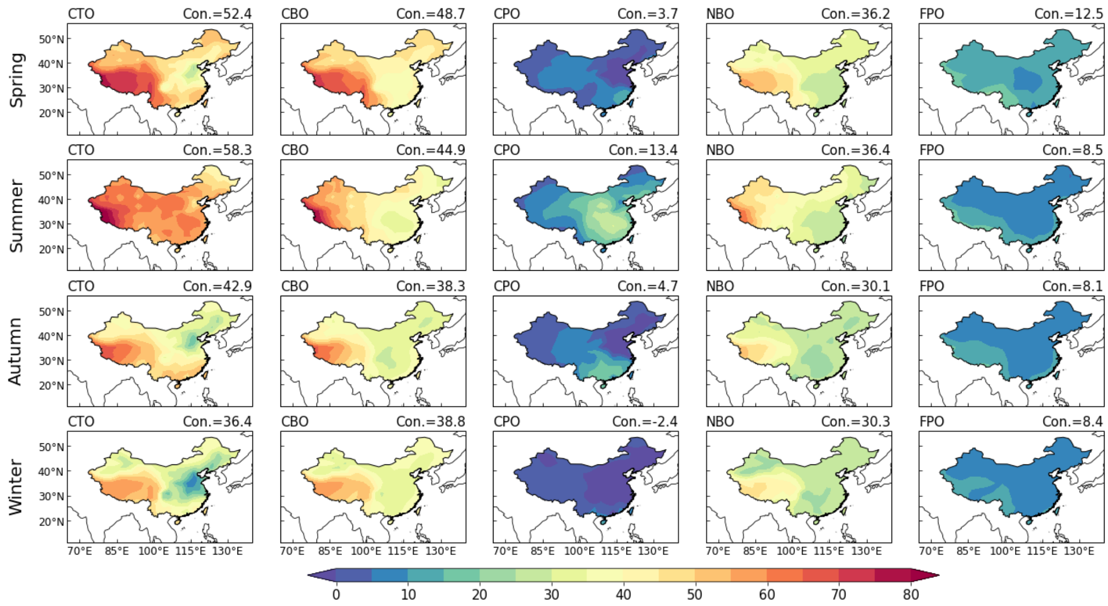

Figure S2. Spatial distributions of seasonal mean CTO, CBO, CPO, NBO and FPO in PD (Units: ppbv). The national mean value is shown in top right of each panel.

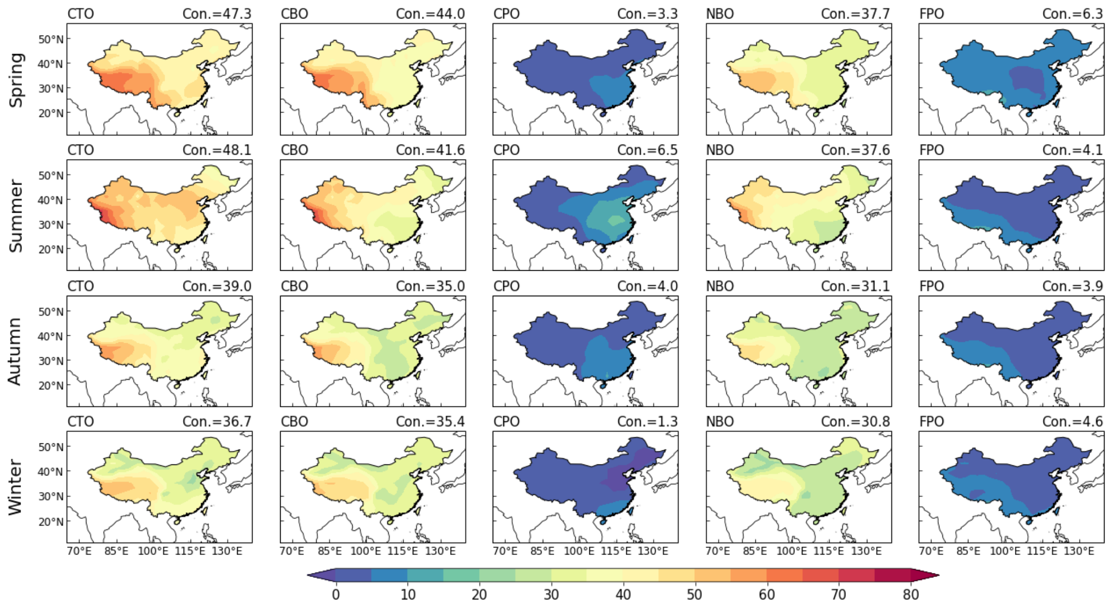

Figure S3. Spatial distributions of seasonal mean CTO, CBO, CPO, NBO and FPO in MC under SSP1-1.9 (Units: ppbv). The national mean value is shown in top right of each panel.

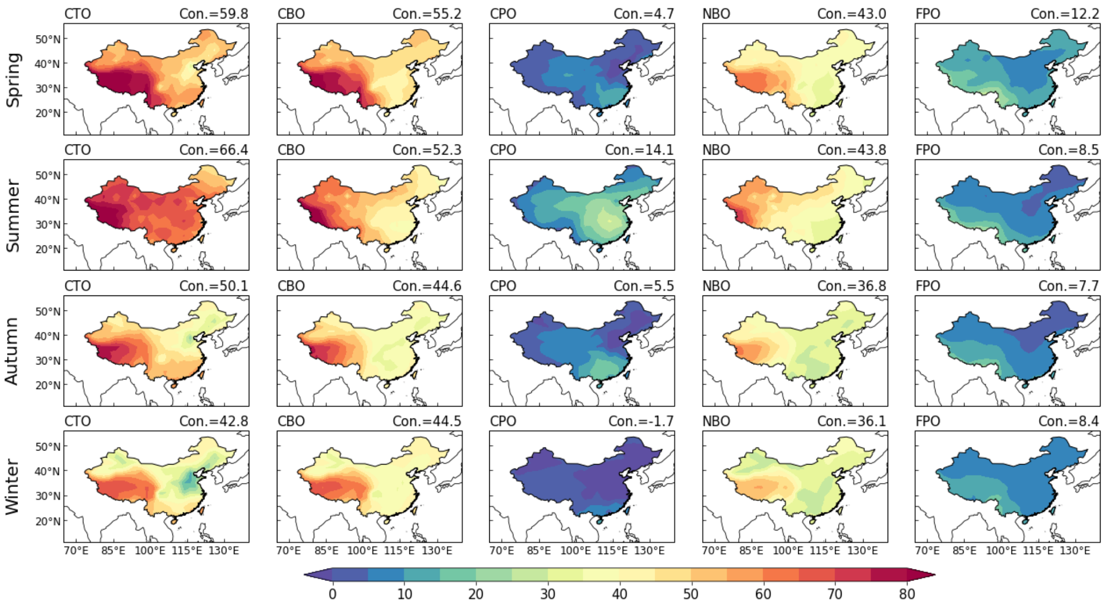

Figure S4. Spatial distributions of seasonal mean CTO, CBO, CPO, NBO and FPO in MC under SSP5-8.5 (Units: ppbv). The national mean value is shown in top right of each panel.

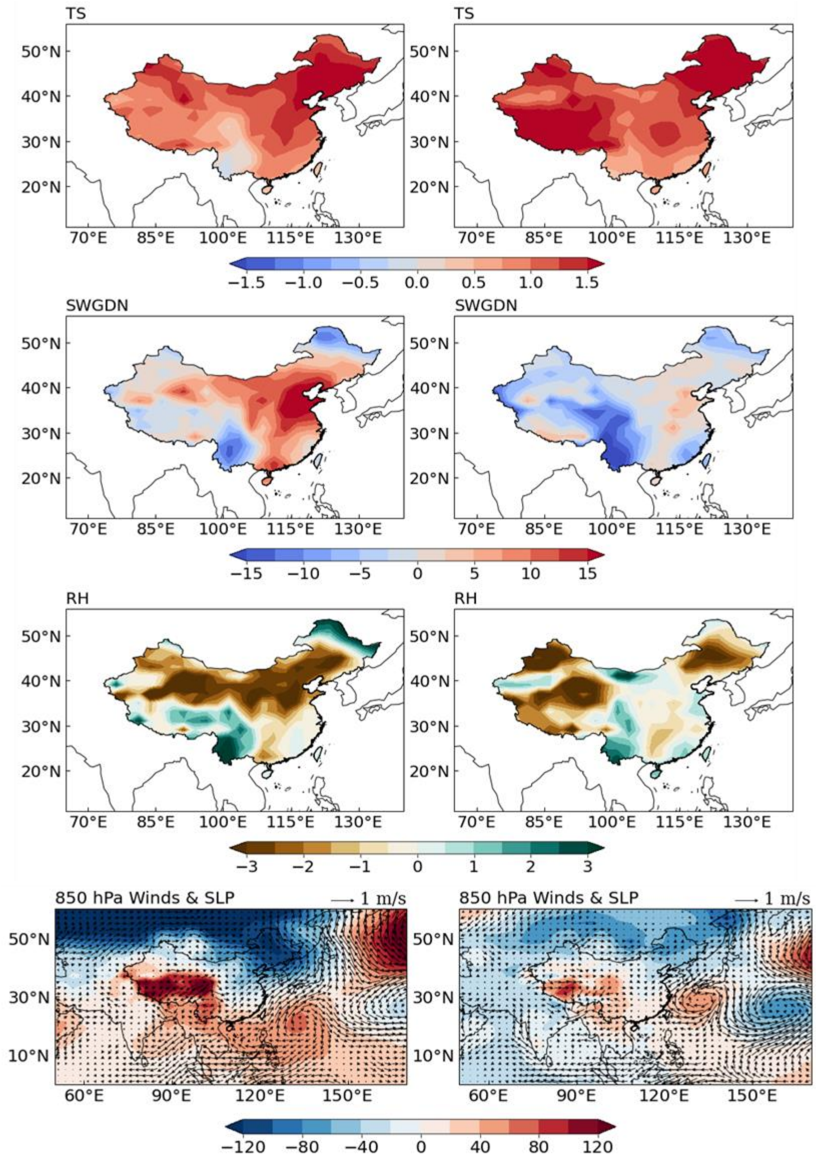

Figure S5. The differences in temperature at surface (TS, units: K), surface incoming shortwave flux (SWGDN, units: W m^{-2}), relative humidity (RH, units: %), and wind fields at 850 hPa (vectors, units: m s^{-1}) and sea-level pressure (contour, units: hPa) in MC under the SSP1-1.9 (left) and SSP5-8.5 (right) scenarios relative to PD.

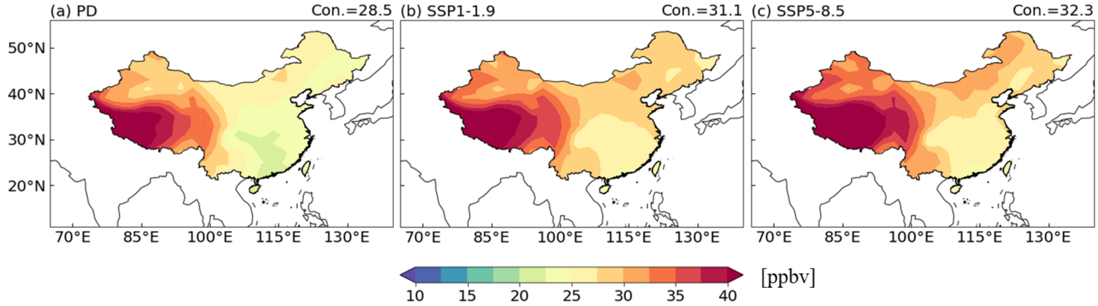

Figure S6. The spatial distribution of pre-industrial natural background ozone (PNB) in (a) PD, and MC under (b) SSP1-1.9, and (c) SSP5-8.5 (Units: ppbv).

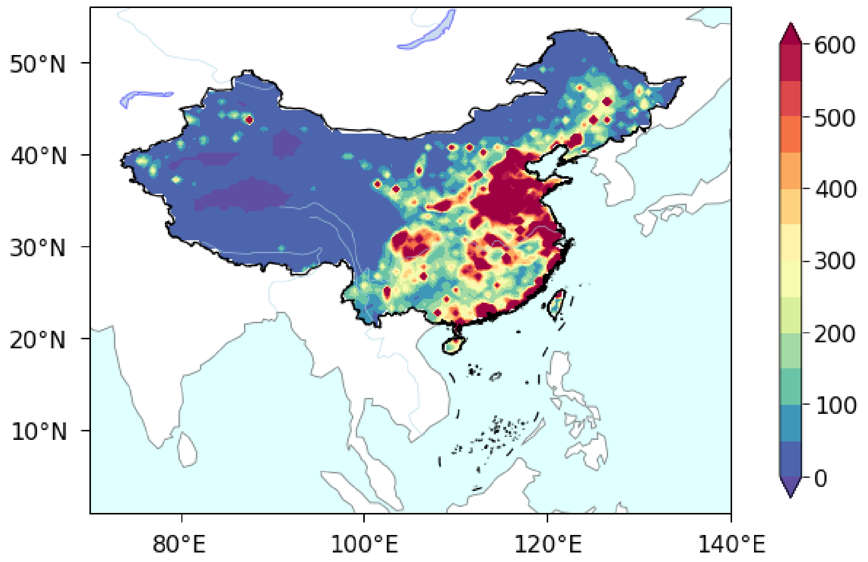

Figure S7. Spatial distribution of population density across China in 2015. Data are from the Gridded Population of the World version 4 (GPWv4) dataset (https://www.earthdata.nasa.gov/data/projects/gpw). Units: persons/km².

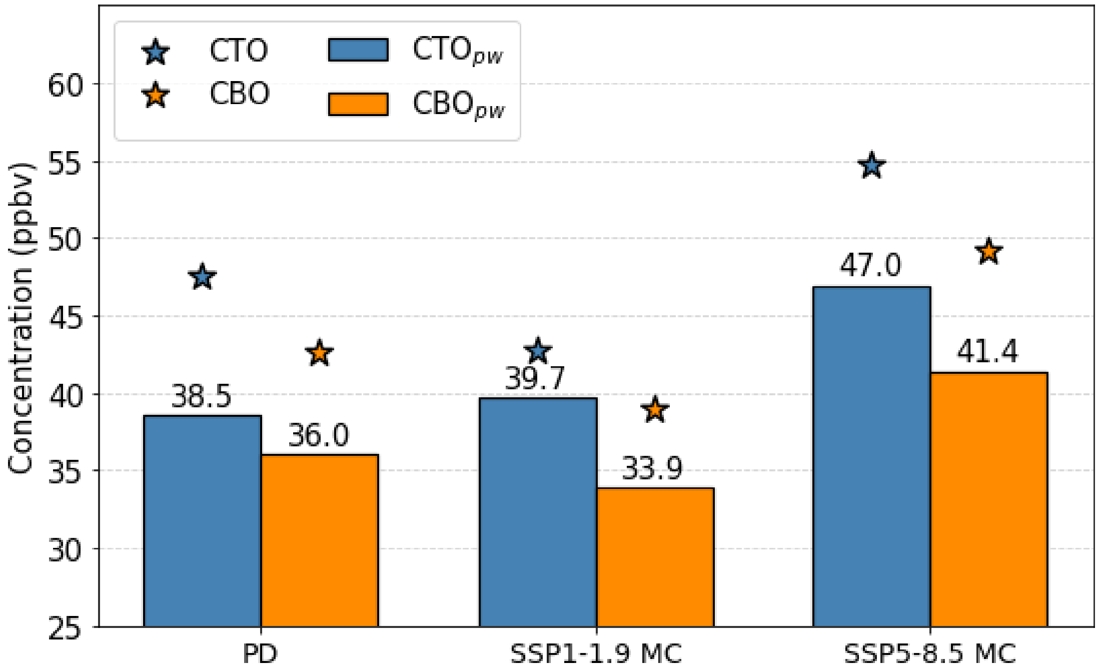

Figure S8. Population-weighted concentrations of CTO (CTO_{PW}, blue bars) and CBO (CBO_{PW}, orange bars) in PD and in MC under SSP1-1.9 and SSP5-8.5. Numerical values above bars indicate population-weighted concentrations. The Stars indicate area-averaged concentrations. Units: ppbv.

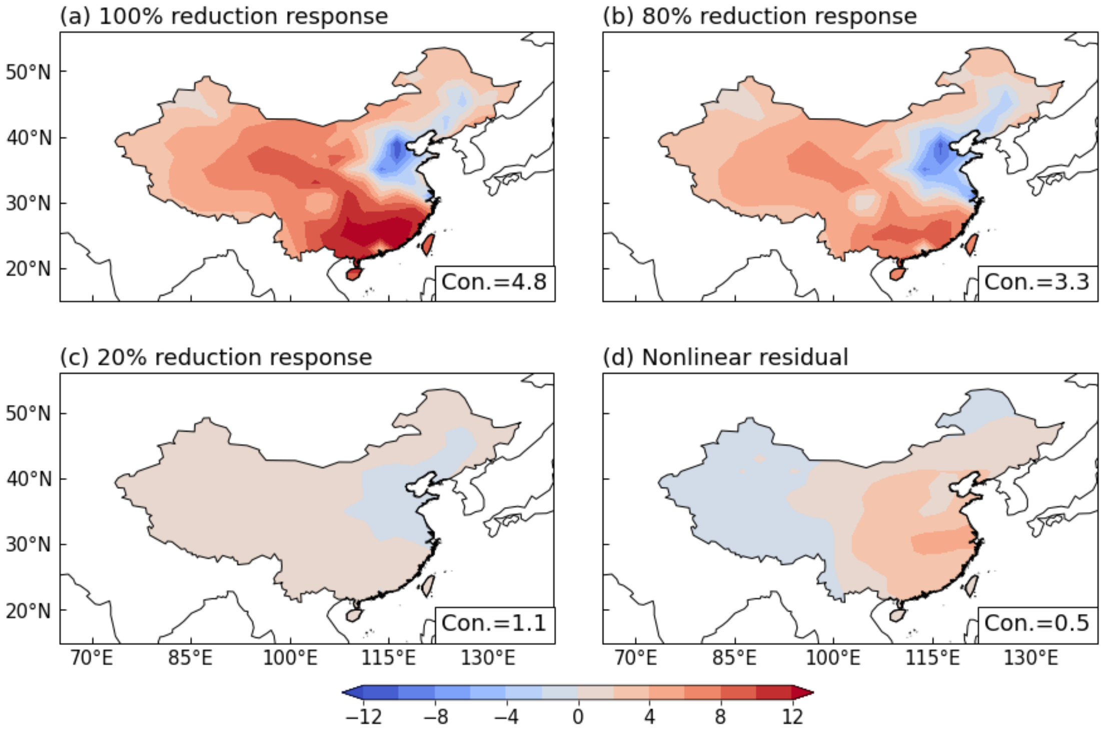

Figure S9. Spatial distribution of changes in ozone concentrations (ppbv) with (a) 100%, (b) 80%, and (c) 20% domestic emission reduction perturbations relative to the baseline (0% domestic emission reduction), and (d) the nonlinear residual, calculated as the difference between (a) and the sum of (b) and (c). (Units: ppbv)

References

Chen, C., Chen, W., Guo, L., Wu, Y., Duan, X., Wang, X., and Shao, M.: A comprehensive review of tropospheric background ozone: Definitions, estimation methods, and meta-analysis of its spatiotemporal distribution in China, https://doi.org/10.5194/egusphere-2025-687, 28 March 2025.

Liu, N., Lin, W., Ma, J., Xu, W., and Xu, X.: Seasonal variation in surface ozone and its regional characteristics at global atmosphere watch stations in China, J. Environ. Sci., 77, 291–302, https://doi.org/10.1016/j.jes.2018.08.009, 2019.

Ma, Z., Xu, J., Quan, W., Zhang, Z., Lin, W., and Xu, X.: Significant increase of surface ozone at a rural site, north of eastern China, Atmos. Chem. Phys., 16, 3969–3977, https://doi.org/10.5194/acp-16-3969-2016, 2016.

Shen, J., He, L., Cheng, P., Xie, M., Jiang, M., Chen, D., and Zhou, G.: Characteristics of ozone concentration variation in the northern background site of the Pearl River Delta, Ecology and Environmental Sciences, 28, 2006–2011, https://doi.org/10.16258/j.cnki.1674-5906.2019.10.010, 2019.

Su, B.: Characteristics and impact factors of O3 concentrations in mountain background region of East China, Environm. Sci., 34, 2519–2525, https://doi.org/10.13227/j.hjkx.2013.07.023, 2013.

Wu, X., Xu, L., Hong, Y., Chen, J., Qiu, Y., Hu, B., Hong, Z., Zhang, Y., Liu, T., Chen, Y., Bian, Y., Zhao, G., Chen, J., and Li, M.: The air pollution governed by subtropical high in a coastal city in Southeast China: Formation processes and influencing mechanisms, Science of The Total Environment, 692, 1135–1145, https://doi.org/10.1016/j.scitotenv.2019.07.341, 2019.

Xu, W., Lin, W., Xu, X., Tang, J., Huang, J., Wu, H., and Zhang, X.: Long-term trends of surface ozone and its influencing factors at the Mt Waliguan GAW station, China – Part 1: Overall trends and characteristics, Atmos. Chem. Phys., 16, 6191–6205, https://doi.org/10.5194/acp-16-6191-2016, 2016.

Xu, X., Lin, W., Xu, W., Jin, J., Wang, Y., Zhang, G., Zhang, X., Ma, Z., Dong, Y., Ma, Q., Yu, D., Li, Z., Wang, D., and Zhao, H.: Long-term changes of regional ozone in China: Implications for human health and ecosystem impacts, Elementa-Sci. Anthrop., 8, 13, https://doi.org/10.1525/elementa.409, 2020.

Zhang, Y., Jin, J., Yan, P., Tang, J., Fang, S., Lin, W., Lou, M., Liang, M., Zhou, Q., Jing, J., Li, Y., Jia, X., and Lyu, S.: Long-term variations of major atmospheric compositions observed at the background stations in three key areas of China, Adv. Clim. Chang. Res., 11, 370–380, https://doi.org/10.1016/j.accre.2020.11.005, 2020.